



Resonant Capture and Separatrix Crossing in Dual-Spin Spacecraft

RICHARD HABERMAN

Department of Mathematics, Southern Methodist University, Dallas, TX 75275, U.S.A.

RICHARD RAND

Department of Theoretical and Applied Mechanics, Cornell University, Ithaca, NY 14853, U.S.A.

THOMAS YUSTER

Department of Mathematics, Lafayette College, Easton, PA 18042, U.S.A.

(Received: 30 March 1998; accepted: 14 September 1998)

Abstract. We consider the rotational motion of a spacecraft composed of two bodies which are free to rotate relative to one another about a common shaft S . A motor on one of the bodies provides a small constant internal torque which influences the relative motion of the two bodies, and which may influence the orientation of their common shaft S . *Resonant capture* refers to the phenomenon that the spacecraft may end up in one of several possible orientations, including a nearly flat spin (transverse to S), in addition to the expected simple rotation about S .

The method of averaging is used to treat the original equations of motion, and it is shown that the essential mathematical problem involves *separatrix crossing* in a problem with slowly moving separatrices. Energy changes represented by Melnikov integrals are used to supplement the averaged equations in the neighborhood of the heteroclinic motions. The method is used to predict which initial conditions lead to capture into each of three distinct capture regions. The asymptotic results are compared to those obtained by direct numerical integration of the equations of motion.

Keywords: Resonance, capture, separatrix, spacecraft, Melnikov.

1. Introduction

A dual-spin spacecraft consists of two bodies, called the platform and the rotor, attached to each other by a shaft S about which they can rotate relative to one another, see Figure 1. In addition, the entire assemblage can rotate freely in space. A motor acting along the shaft S may be utilized to apply an equal and opposite torque to both bodies. The motor may be used to control the orientation of the spacecraft in space. In this work we will be concerned with accomplishing a rotational pointing maneuver with a small constant torque supplied by the motor.

We model the platform and rotor as rigid bodies. The rotor is assumed to be axisymmetric and balanced, with its symmetry axis coinciding with the shaft S . The platform is assumed to be asymmetric and balanced. Here *balanced* means that the shaft axis S is a principal axis for the moment of inertia tensor, i.e., no product of inertia terms are present. Also, *axisymmetric* means that all principal moments of inertia in directions orthogonal to S are equal. We assume that the initial state of the system and the physical parameters are chosen such that the applied torque is able to drive the system towards what turns out to be one of three different classes of motions, a process called *resonant capture*. Each of these classes of motions will be shown to

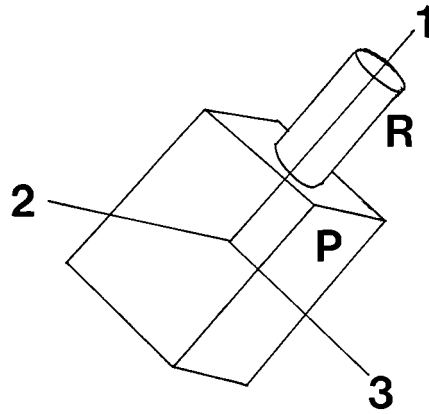


Figure 1. Model of a dual-spin spacecraft consists of an axisymmetric rotor R and an asymmetric platform P . Their common shaft S is directed along axis 1. Axes 1–2–3 are fixed in P .

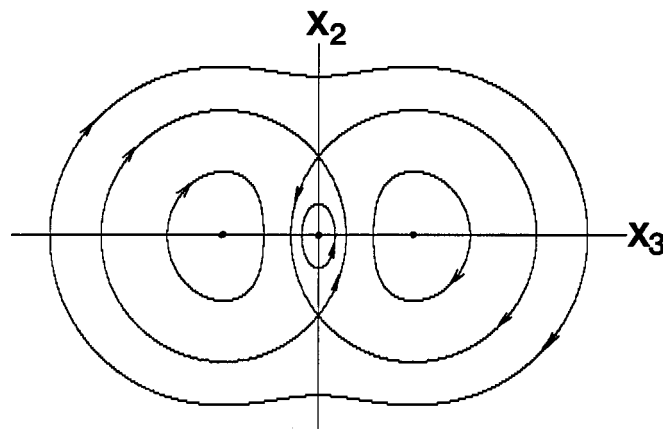


Figure 2. In the parameter range $0 < \mu < -i_2$, $\varepsilon = 0$ (μ fixed), Equations (1–4) exhibit four heteroclinic orbits which connect two saddle points. Displayed is a projection from the North pole of the sphere (7) onto the plane $x_1 = -1$. In addition to the separatrices, four periodic orbits are also shown. Dots represent centers. The origin represents the South pole of the sphere. The North pole lies at infinity in this projection (cf. Figure 3).

lie in *capture regions* which are separated from each other by slowly moving separatrices, see Figure 2. We shall be concerned with predicting which initial conditions lead to capture into each of these capture regions.

Our procedure will be to follow the work of Haberman and his colleagues [2–4, 8], and replace the original equations of motion by averaged equations. The averaging process is not valid in the neighborhood of the slowly moving separatrices, however, and energy changes represented by Melnikov-type integrals are used to handle the problem of *separatrix crossing*.

The problem of resonant capture in dual-spin spacecraft has been studied recently in a number of research papers. Kinsey et al. [15, 16] studied spinup in a dual-spin spacecraft in which the rotor was axisymmetric with small imbalance, while the platform was axisymmetric and balanced. They used the method of averaging to show that some initial conditions lead to *pass-through*, while others lead to capture. Rand et al. [21] and Quinn et al. [18] studied a simpler model problem and showed that capture corresponded to the entry of a given trajectory into a region of phase space bounded by a slowly moving ‘instantaneous separatrix’. In Hall

and Rand [13] the rotor was taken as axisymmetric and balanced, while the platform was asymmetric and balanced. Instead of visualizing the dynamics on a sequence of momentum spheres, they used a two-dimensional space with coordinates of energy and a slowly-varying parameter to display the motion of the system. They obtained averaged equations of motion, which turned out to involve elliptic functions. They noted that numerical integration of the averaged equations was inaccurate in the neighborhood of separatrix crossings, since the averaged equations are not valid near the instantaneous separatrices. Hall [11] used a similar system, reversing the roles played by rotor and platform, to discuss resonant capture during despin of the axisymmetric platform. He presented a probabilistic treatment of capture based on numerical integration of the original (unaveraged) equations. Tsui and Hall [26] used a similar approach to treat the system dealt with by Kinsey et al. [15, 16]. Hall [12] used a similar approach to treat the problem of an asymmetric platform attached to N axisymmetric rotors. He showed that although the problem is described by $N + 3$ first order ordinary differential equations, conservation of angular momentum and the method of averaging could be used to reduce the number of equations to one for small spinup torques. The reader is referred to [12] for an extensive list of related references. All these papers share the essential difficulty of how to handle the crossing of the separatrix. The special feature of the present work is that separatrix crossing is treated using consistent asymptotic approximations via Haberman's approach.

2. Summary of Our Approach

For the reader's convenience we offer the following summary of the approach used in this paper. The process of resonant capture will be shown to consist of the gradual approach towards the separatrix loops of Figure 2 of motions which start outside these separatrices. After circulating around the loops in general many times, a given motion eventually crosses the instantaneous separatrix and enters one of the three separated regions. Just before a motion reaches the instantaneous separatrix, it must pass through a region close to one of the saddles which we will call *the entrance saddle approach*. Using Melnikov integrals, we will be able to compute the energy needed at the entrance saddle approach in order for a given motion to lie on the basin boundaries of the separated regions, i.e. to lie on the stable manifold of the saddle-like *normally hyperbolic motions*. Then we will use equations obtained by the method of averaging, which are valid in the regions away from the separatrices, to determine which initial conditions lead to motions that pass through the entrance saddle approach with the appropriate energy so as to lie on the various basin boundaries.

3. Equations of Motion

We consider a spacecraft consisting of an axisymmetric, balanced rotor and an asymmetric, balanced platform, see Figure 1. The components of the dimensionless angular momentum vector (x_1, x_2, x_3) are referred to axes fixed in the platform with principal axis $(1, 0, 0)$ directed along the shaft S , and with perpendicular axes $(0, 1, 0)$ and $(0, 0, 1)$ also corresponding to principal axes for the spacecraft. We present the following equations of motion without derivation. For a derivation, see [13, 14].

$$\frac{dx_1}{dt} = (i_2 - i_3)x_2x_3, \tag{1}$$

$$\frac{dx_2}{dt} = (i_3x_1 - \mu)x_3, \quad (2)$$

$$\frac{dx_3}{dt} = -(i_2x_1 - \mu)x_2, \quad (3)$$

$$\frac{d\mu}{dt} = -\varepsilon, \quad (4)$$

where

$$x_i = h_i/h, \quad i = 1, 2, 3,$$

$$h = \sqrt{h_1^2 + h_2^2 + h_3^2},$$

$$h_1 = I_1\omega_1 + I_s\omega_s,$$

$$h_2 = I_2\omega_2, h_3 = I_3\omega_3,$$

$$I_i = \text{moment of inertia of spacecraft about axis } i, \quad i = 1, 2, 3,$$

$$I_s = \text{moment of inertia of rotor about axis 1 (shaft } S),$$

$$\omega_i = \text{angular velocity of platform about axis } i, \quad i = 1, 2, 3,$$

$$\omega_s = \text{angular velocity of rotor about axis 1 (shaft } S),$$

$$i_j = 1 - I_p/I_j, \quad j = 2, 3,$$

$$I_p = I_1 - I_s = \text{moment of inertia of platform about axis 1 (shaft } S),$$

$$\mu = h_a/h = \text{dimensionless angular momentum of rotor about axis 1 (shaft } S),$$

$$h_a = I_s(\omega_s + \omega_1) = \text{angular momentum of rotor about axis 1 (shaft } S),$$

$$t = h\tilde{t}/I_p = \text{scaled time,}$$

$$\tilde{t} = \text{real time,}$$

$$\varepsilon = g_a I_p/h^2,$$

$$g_a = \text{despin torque applied by platform on rotor about the negative 1 axis (shaft } S).$$

Note that the assumption of constant torque g_a in Equation (4) gives

$$\mu = \mu_0 - \varepsilon t. \quad (5)$$

We shall generalize this to

$$\mu = \mu(\varepsilon t), \quad \frac{d\mu}{dt} < 0. \quad (6)$$

Multiplying Equations (1–3), respectively by x_1, x_2, x_3 and adding shows that angular momentum is conserved (even when μ is not constant) in the form:

$$x_1^2 + x_2^2 + x_3^2 = \text{constant} = 1, \quad (7)$$

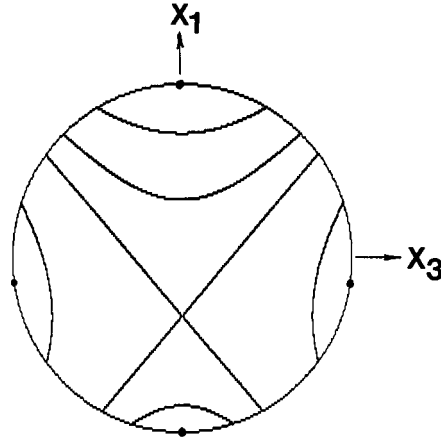


Figure 3. Orbits of Equations (1–4) for $\mu = 0.1$, $\varepsilon = 0$ (μ fixed), a projection of the sphere (7) from infinity onto the x_3 - x_1 plane. Dots represent centers. The separatrices of Figure 2 appear here as two intersecting straight lines. Periodic orbits encircling each of the centers appear as curved line segments.

where the constant of integration is unity in view of the definition of dimensionless angular momentum $x_i = h_i / \sqrt{h_1^2 + h_2^2 + h_3^2}$. In this paper we analyze the dynamical system (1–3), (6) on the unit sphere (7).

We begin by briefly reviewing some features of the system when μ is constant (see [13] for more details). As in [13] we shall treat oblate spacecrafts for which $I_p > I_2 > I_3$, or, equivalently, $i_3 < i_2 < 0$. E.g., looking ahead towards our numerical example, we shall take $i_3 = -0.7$ and $i_2 = -0.3$. Equations (1–3) possess two, four or six equilibria, depending on the value of μ . In the range we shall be interested in, $0 < \mu < -i_2$, there are six equilibria on the sphere (7), four centers and two saddle points, see Figure 3. There are centers at the North $(1, 0, 0)$ and South $(-1, 0, 0)$ poles. There are two more centers located symmetrically in x_3 at $x_1 = \mu/i_3$, $x_2 = 0$, $x_3^2 = 1 - (\mu/i_3)^2$. The saddle points are located at $x_1 = \mu/i_2$, $x_2^2 = 1 - (\mu/i_2)^2$, $x_3 = 0$. There are four heteroclinic orbits which connect the two saddle points as shown in Figures 2 and 3. As shown in [13], a pitchfork bifurcation occurs at $\mu = -i_2$ ($= 0.3$ here) in which the two saddles coalesce with the center at the South pole, creating a saddle there. Another pitchfork occurs at $\mu = -i_3$ ($= 0.7$ here) in which the two symmetrical centers combine with the saddle at the South pole to create a center there.

When μ is constant, Equations (1–3) admit the following energy-like integral (which we call H after the Hamiltonian, even though this system will be shown not to be Hamiltonian)

$$H = -2\mu x_1 + i_3 x_1^2 + (i_3 - i_2)x_2^2 - i_3 + i_2 + \frac{\mu^2}{i_2}. \quad (8)$$

We have chosen the constant in Equation (8) so that H is zero at the saddle points. The Hamiltonian (energy) is positive in the regions immediately surrounding the North and South poles, while the energy is negative in regions immediately surrounding the symmetric centers. Thus, for constant μ , all the solutions are periodic, corresponding to closed curves on the sphere, except for the heteroclinic orbits.

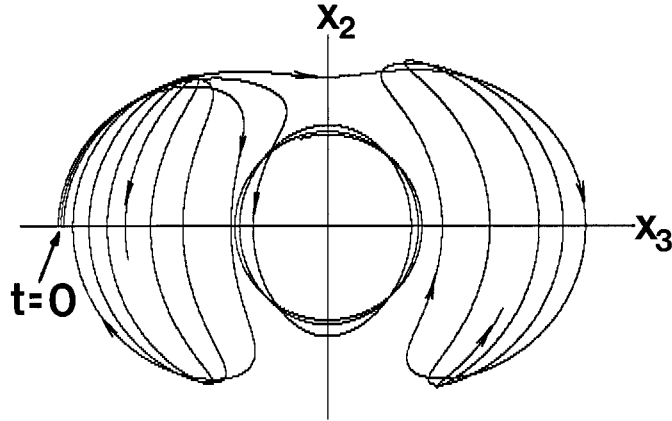


Figure 4. Numerical integration of Equations (1–4) showing how three different initial conditions lead to capture into each of three capture regions. Parameters are $i_2 = -0.3$, $i_3 = -0.7$, $\varepsilon = 0.003$, $\mu_0 = 0.25$. Initial conditions are $x_2(0) = 0$ and $x_3(0) = -0.945$, -0.955 , and -0.965 , and $x_1(0) > 0$ given by Equation (7). Each initial condition produces a trajectory which is respectively captured into the left, middle and right capture regions. Projection is from infinity onto the x_3 - x_2 plane.

The foregoing conclusions no longer hold true when μ is permitted to change slowly in time. In this case H ceases to be a first integral and varies according to

$$\frac{dH}{dt} = -2 \frac{d\mu}{dt} \left(x_1 - \frac{\mu}{i_2} \right). \quad (9)$$

The points on the sphere which were equilibria for constant μ in general cease to be equilibria when μ changes slowly, and will be referred to as *slowly-varying equilibria*. The North and South poles of the sphere are exceptions and remain true equilibria even when μ changes in time. The saddle points are structurally stable features, and for small $(d\mu)/(dt)$ the slowly-varying saddles give rise to saddle-like normally hyperbolic motions. The slowly-varying centers, however, will in general lose their center-like quality and will become hyperbolic.

The dynamics of the system (1–4) turn out to involve a competition between the three regions associated with each of the slowly-varying centers, see Figure 4. Our goal in this work is to determine which initial conditions lead to capture into each of these regions.

4. Energy-Angle Coordinates

In order to conveniently apply the method of averaging to this problem, we change variables to what we call *energy-angle coordinates* (similar to, but not the same as action-angle variables). This is accomplished by first reducing the three-dimensional system (1–3), to a two-dimensional system with coordinates x_1 and x_2 by using Equation (7) to eliminate x_3 .

We rewrite Equations (1) and (2) in the form

$$\frac{dq}{dt} = f_1(q, p, T) + \varepsilon g_1(q, p, T), \quad (10)$$

$$\frac{dp}{dt} = f_2(q, p, T) + \varepsilon g_2(q, p, T), \quad (11)$$

where

$$q = x_1, \quad p = x_2, \quad T = \varepsilon t,$$

$$f_1 = (i_2 - i_3)x_2x_3 = (i_2 - i_3)px_3(q, p),$$

$$f_2 = (i_3x_1 - \mu)x_3 = (i_3q - \mu)x_3(q, p),$$

$$g_1 = g_2 = 0, \text{ included here to make the analysis more general.}$$

Equations (10) and (11) can be made to resemble a Hamiltonian system by noting that

$$f_1 = \gamma H_p, \tag{12}$$

$$f_2 = -\gamma H_q, \tag{13}$$

where

$$\gamma = -x_3(q, p)/2. \tag{14}$$

Note that the general formulation (10) and (11) with (12) and (13) includes the case where the unperturbed system is Hamiltonian (if γ is a constant). This is not the case for Equations (1), (2), (3), however.

Now we transform to energy-angle coordinates (H, ψ) . We normalize the angle or phase so that the coordinates (q, p) repeat when ψ is increased by one. The coordinate system is defined by the unperturbed problem with μ fixed. The angle ψ is defined by

$$\frac{\psi}{\omega(H, T)} = \int_{q_c(H, T)}^q \frac{d\bar{q}}{f_1(\bar{q}, \bar{p}, T)} = \int_{p_c(H, T)}^p \frac{d\bar{p}}{f_2(\bar{q}, \bar{p}, T)}, \tag{15}$$

where $\omega(H, T)$ is the frequency related to the usual period of the nonlinear oscillator involving the closed line integral \oint :

$$\frac{1}{\omega(H, T)} = \oint \frac{d\bar{q}}{f_1(\bar{q}, \bar{p}, T)} = \oint \frac{d\bar{p}}{f_2(\bar{q}, \bar{p}, T)}. \tag{16}$$

The integrals are performed with H and T fixed. The lower limits correspond to where we choose $\psi = 0$. Given H and ψ , $q = q(\psi, H, T)$ and $p = p(\psi, H, T)$ are determined from Equation (15) and are periodic in ψ (with period 1). By taking $\partial/(\partial\psi)$ of Equation (15), we obtain the exact equations

$$\omega q_\psi = f_1(q, p, T), \tag{17}$$

$$\omega p_\psi = f_2(q, p, T). \tag{18}$$

In Appendix A, we use the chain rule for partial derivatives to derive the transformed equations of motion:

$$\frac{dH}{dt} = \varepsilon(g_1H_q + g_2H_p + H_T), \tag{19}$$

$$\frac{d\psi}{dt} = \omega(H, T) + \varepsilon(g_1\psi_q + g_2\psi_p + \psi_T). \tag{20}$$

For the dual-spin spacecraft problem (1–3) and (6), we have $g_1 = g_2 = 0$ and Equations (8) and (9) give

$$\frac{dH}{dt} = -2\varepsilon\mu_T \left(q - \frac{\mu}{i_2} \right), \quad (21)$$

$$\frac{d\psi}{dt} = \omega(H, T) + \varepsilon\psi_T. \quad (22)$$

Even though we will be working to higher order in ε , it turns out that we will not need to know much about ψ_T .

5. Symmetries

Our results require the use of particularly accurate averaged equations which depend on certain symmetries with respect to the phase angle ψ of the system as they apply especially to the perturbations in Equations (19) and (20). We, therefore, examine the symmetries of the system. Symmetry in $p = x_2$ will be very important for us. We note that the Hamiltonian given by Equation (8) is symmetric in $p = x_2$, by which we mean $H(q, -p, T) = H(q, p, T)$. When the Hamiltonian is symmetric we choose $\psi = 0$ at $p = 0$ (usually the minimum of q), and thus the lower limit of integration $p_c(H, T) = 0$ in Equation (15). In general, we need $f_1(q, p, T)$ to be an odd function of p and $f_2(q, p, T)$ to be an even function of p . This requires that $\gamma(q, p, T)$ be an even function of p , a condition which we assume is valid. In the case of the present application, Equations (14) and (7) give $\gamma = \pm\sqrt{1 - q^2 - p^2}/2$, an even function of p . From the phase portrait,

$$p \text{ is an odd function of } \psi, \quad (23)$$

(and q is an even function of ψ). Any even function of p will be an even function of ψ , and any odd function of p will be an odd function of ψ . First partial derivatives with respect to p of an even function of p will be an odd function of p (and vice versa). Partial derivatives with respect to q and T hold p fixed and hence even functions of p stay even (and vice versa). Thus

$$H \text{ is an even function of } p \text{ (} H \text{ is an even function of } \psi), \quad (24)$$

$$H_p \text{ is an odd function of } p \text{ (} H_p \text{ is an odd function of } \psi), \quad (25)$$

$$H_q \text{ is an even function of } p \text{ (} H_q \text{ is an even function of } \psi), \quad (26)$$

$$H_T \text{ is an even function of } p \text{ (} H_T \text{ is an even function of } \psi). \quad (27)$$

Since p is an odd function of ψ , it follows that

$$\psi \text{ is an odd function of } p \text{ (} \psi \text{ is an odd function of } \psi), \quad (28)$$

$$\psi_p \text{ is an even function of } p \text{ (} \psi_p \text{ is an even function of } \psi), \quad (29)$$

$$\psi_q \text{ is an odd function of } p \text{ (} \psi_q \text{ is an odd function of } \psi), \quad (30)$$

$$\psi_T \text{ is an odd function of } p \text{ (} \psi_T \text{ is an odd function of } \psi). \quad (31)$$

The evenness and oddness of various derivatives with respect to ψ can also be derived using the expressions for them in Appendix A.

We assume the perturbation $\varepsilon g_1(q, p, T)$ is an even function of p , and we assume $\varepsilon g_2(q, p, T)$ is an odd function of p . These are the same kind of symmetries that arise for damping in a conservative system, so that Bourland and Haberman [2] have referred to this type of perturbation as ‘purely dissipative’ (see also [8]). Thus,

$$g_1 \text{ is an even function of } p \text{ (} g_1 \text{ is an even function of } \psi), \quad (32)$$

$$g_2 \text{ is an odd function of } p \text{ (} g_2 \text{ is an odd function of } \psi). \quad (33)$$

We put the energy-angle equations (19) and (20) in what is called standard form [1, 23]:

$$\frac{dH}{dt} = \varepsilon f(H, \psi, T), \quad (34)$$

$$\frac{d\psi}{dt} = \omega(H, T) + \varepsilon g(H, \psi, T), \quad (35)$$

where

$$f = g_1 H_q + g_2 H_p + H_T, \quad (36)$$

$$g = g_1 \psi_q + g_2 \psi_p + \psi_T. \quad (37)$$

Using Equations (24–33), it immediately follows that the $O(\varepsilon)$ terms in standard form have the following symmetry:

$$f \text{ is an even function of } p \text{ (} f \text{ is an even function of } \psi), \quad (38)$$

$$g \text{ is an odd function of } p \text{ (} g \text{ is an odd function of } \psi). \quad (39)$$

In the present application $f = -2\mu_T(q - (\mu/i_2))$ and $g = \psi_T$, which has the desired symmetry due to Equation (31).

6. Averaging

In this section, we follow the procedure used in [2, 8] to apply the method of averaging to the energy-angle equations (34) and (35). The method of averaging allows us to investigate the effect of slow variation of parameters, and of other perturbations, on the behavior of the system for long times ($t = O(1/\varepsilon)$, $T = \varepsilon t = O(1)$) by averaging over the faster motion of the unperturbed system. We will use higher-order averaging [1, 19, 20, 23] which involves transforming the governing Equations (34) and (35) to a simpler form via a near-identity transformation:

$$H = e + \varepsilon H_1(e, \phi, T) + \varepsilon^2 H_2(e, \phi, T) + \dots, \quad (40)$$

$$\psi = \phi + \varepsilon \psi_1(e, \phi, T) + \varepsilon^2 \psi_2(e, \phi, T) + \dots, \quad (41)$$

where H_i and ψ_i are periodic functions of ϕ . Here e and ϕ are the transformed or averaged versions of H and ψ . We will require that $\int_0^1 H_i(e, \phi, T) d\phi = 0$ so that e is the average of the energy H . We also choose $\int_0^1 \psi_i(e, \phi, T) d\phi = 0$.

In Appendix B we show that when Equations (40) and (41) are introduced into Equations (34) and (35), the resulting equations on e and ϕ become:

$$\frac{de}{dt} = \varepsilon(f - \omega H_{1_\phi}) + \varepsilon^2(M - \omega H_{2_\phi}) + O(\varepsilon^3), \quad (42)$$

$$\frac{d\phi}{dt} = \omega(e, T) + \varepsilon(g - \omega \psi_{1_\phi} + \omega_e H_1) + O(\varepsilon^2), \quad (43)$$

where

$$M = -\omega_e H_1 H_{1_\phi} + f_e H_1 + f_\phi \psi_1 - f H_{1_e} - g H_{1_\phi} + \omega H_{1_\phi} (H_{1_e} + \psi_{1_\phi}) - H_{1_T}. \quad (44)$$

The right-hand sides of Equations (42) and (43) are periodic functions of ϕ . It follows that $(de)/(dt)$ and $(d\phi)/(dt)$ satisfy the averaged equations

$$\frac{de}{dt} = \varepsilon \langle f \rangle + \varepsilon^2 \langle M \rangle + O(\varepsilon^3), \quad (45)$$

$$\frac{d\phi}{dt} = \omega(e, T) + \varepsilon \langle g \rangle + O(\varepsilon^2), \quad (46)$$

where we have introduced the notation $\langle f \rangle = \int_0^1 f d\phi$ for the average (mean) of any function f for fixed e and T . We have noted that for example $\langle H_{1_\phi} \rangle = 0$ because H_1 is periodic in ϕ , and we have assumed that H_1 has zero average. It will be helpful to introduce the fluctuating (or oscillatory) part of a periodic function defined to be the difference between it and its average:

$$\{f\} = f - \langle f \rangle. \quad (47)$$

By comparing Equations (42) and (43) to Equations (45) and (46), we find equations that define the near identity transformations

$$\omega H_{1_\phi} = \{f\}, \quad (48)$$

$$\omega H_{2_\phi} = \{M\}, \quad (49)$$

$$\omega \psi_{1_\phi} = \{g + \omega_e H_1\}. \quad (50)$$

In order for H_1 to have zero average, we integrate Equation (48) and obtain

$$H_1 = \frac{1}{\omega} \int_0^\phi \{f\} d\phi' - \frac{1}{\omega} \left\langle \int_0^\phi \{f\} d\phi' \right\rangle. \quad (51)$$

Since from Equation (38) f is an even periodic function of ϕ , it follows that $\{f\}$ is an even periodic function with zero average. Thus, $\int_0^\phi \{f\} d\phi'$ is an odd periodic function, which

therefore has zero average, $\langle \int_0^\phi \{f\} d\phi' \rangle = 0$. Thus H_1 is an odd periodic function of ϕ satisfying

$$H_1 = \frac{1}{\omega} \int_0^\phi \{f\} d\phi'. \quad (52)$$

Expressions for H_2 and ψ_1 exist but we do not need them in this paper.

Symmetry results that we need are

$$H_1 \text{ is an odd function of } \phi, \quad (53)$$

$$H_{1_\phi} \text{ is an even function of } \phi, \quad (54)$$

$$H_{1_e} \text{ is an odd function of } \phi, \quad (55)$$

$$H_{1_T} \text{ is an odd function of } \phi. \quad (56)$$

We also need symmetry results for ψ_1 which can be obtained from Equation (50). Since H_1 from Equation (53) and g from Equation (39) are odd functions of ϕ , it follows that

$$\psi_1 \text{ is an even function of } \phi, \quad (57)$$

$$\psi_{1_\phi} \text{ is an odd function of } \phi. \quad (58)$$

We now simplify Equations (45) and (46). From Equation (39) g is an odd function of ϕ , and thus $\langle g \rangle = 0$. From Equations (38), (39) and (53–58), it follows that M defined by Equation (44) is an odd periodic function of ϕ , and hence $\langle M \rangle = 0$. The leading-order equations for the averaged energy and phase are accurate to higher-order (using the symmetry arguments) in the sense that

$$\frac{de}{dt} = \varepsilon \langle f \rangle + O(\varepsilon^3), \quad (59)$$

$$\frac{d\phi}{dt} = \omega(e, T) + O(\varepsilon^2). \quad (60)$$

Using Equation (17), we have

$$\langle f \rangle = \omega(e, T) \oint \frac{f d\bar{q}}{f_1(\bar{q}, \bar{p}, T)}, \quad (61)$$

where from Equation (36) and the near-identity transformation we have:

$$f = g_1 e_q + g_2 e_p + e_T. \quad (62)$$

The integral in Equation (61) should be computed at fixed e and T , so that

$$\langle f \rangle = -\omega(e, T) D(e, T), \quad (63)$$

where the dissipation integral $D(e, T)$ is defined by

$$D(e, T) = - \oint \frac{f d\bar{q}}{f_1(\bar{q}, \bar{p}, T)}. \quad (64)$$

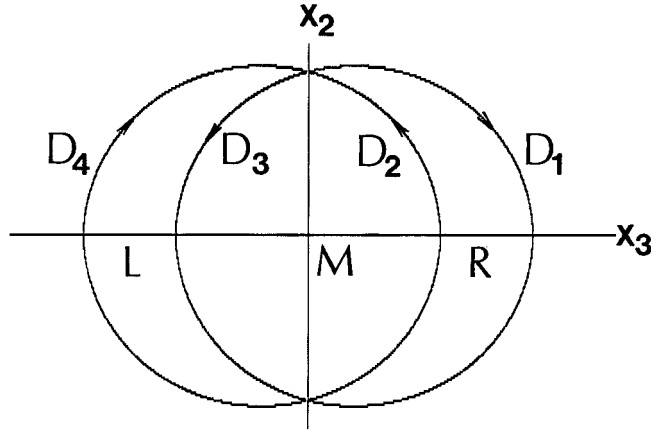


Figure 5. The four heteroclinic parameters D_i of Equation (67) are Melnikov integrals. The capture regions L, M and R are marked. The origin here corresponds to the South pole of the sphere (7), and to motion of the spacecraft about the common shaft S . Capture into regions L and R corresponds to more general motions of the spacecraft, including the possibility of a flat spin, that is, a motion transverse to S .

Here $D(e, T)$ is approximately the change in energy over one periodic orbit. In the dual-spin spacecraft example, Equation (1) gives $f_1 = (i_2 - i_3)x_2x_3 = (i_2 - i_3)px_3(q, p)$ and Equation (21) gives

$$f = e_T = -2\mu_T \left(q - \frac{\mu}{i_2} \right). \quad (65)$$

We have shown that the leading-order averaged energy and angle equations (59) and (60) obtained by the method of averaging are more accurate than one would have anticipated. These averaged equations are valid away from the separatrices of the unperturbed problem. However, as the slowly varying strongly nonlinear oscillatory orbits approach an unperturbed heteroclinic orbit, the method of averaging fails. Nevertheless, we will show in the next section how the averaged equations may be supplemented in order to calculate the boundaries of the basin of attraction.

7. Separatrix Crossing

The method of averaging fails near an unperturbed heteroclinic orbit because the period of oscillation approaches infinity. The unperturbed heteroclinic orbits have been defined by $e = 0$. The slow variation Equation (59) predicts a slow time $T_c = \varepsilon t_c$ at which an unperturbed heteroclinic orbit is passed. Since it is known [24] that the time between saddle approaches is logarithmically large $O(\ln \varepsilon)$ on the fast scale t but small $O(\varepsilon \ln \varepsilon)$ on the slow time scale $T = \varepsilon t$, the slow time variable may be frozen at T_c as an approximation valid for passage through the unperturbed heteroclinic orbit. This is valid even though the time predicted for crossing the unperturbed heteroclinic orbit by slow variation theory is not valid. See [2] where it is shown that the time error is $O(1)$ in the fast time variable t , but is small in the slow time variable $T = \varepsilon t$.

To analyze nearly heteroclinic orbits, we use techniques originally developed for nearly homoclinic orbits. Timofeev [25], Tennyson et al. [24], and Bourland and Haberman [2] showed

that the slow passage through an unperturbed homoclinic orbit consists of a large sequence of nearly homoclinic orbits. For our case, the solution consists of a large sequence of nearly heteroclinic orbits whose phase portrait is shown in Figure 5. Well-known methods for nearly homoclinic orbits may be used. Along these nearly heteroclinic orbits (see, for example, [6]), the leading order change (dissipation) in the energy H over a complete orbit from one saddle approach to the next can be approximated by the heteroclinic *Melnikov function* (calculated along an unperturbed heteroclinic orbit):

$$\Delta H \approx \varepsilon \int_{-\infty}^{\infty} (g_1 H_q + g_2 H_p + H_T) dt = \int \frac{(g_1 H_q + g_2 H_p + H_T) d\bar{q}}{f_1(\bar{q}, \bar{p}, T)}, \quad (66)$$

where $f_1 = H_p \gamma$. Extensions like Equation (66) for problems with slow variation were described in [7, 22].

This leads us to define four different heteroclinic parameters D_1, D_2, D_3, D_4 , as path integrals along the four different heteroclinic orbits, see Equations (36) and (64) and Figure 5:

$$D_i = - \int \frac{(g_1 H_q + g_2 H_p + H_T) d\bar{q}}{f_1(\bar{q}, \bar{p}, T)}. \quad (67)$$

In the case of slow variation these integrals depend on T but as described in the previous paragraph can be frozen at T_c predicted by slow variation theory. Note that the dissipation integral for nonlinear oscillators approaches the appropriate sum of the heteroclinic dissipation functions. Since the energy is positive in the region marked M in Figure 5, but the energy is negative in the regions marked L and R, in order for motions to be able to be captured into each of the three capture regions, the following restrictions must be satisfied by the heteroclinic dissipation parameters:

$$D_3 + D_4 > 0, \quad (68)$$

$$D_1 + D_2 > 0, \quad (69)$$

$$D_2 + D_3 < 0. \quad (70)$$

By adding Equations (68) and (69) and comparing that with Equation (70), it follows that

$$D_1 + D_4 > 0, \quad (71)$$

so that the periodic orbits which surround the three capture regions (see Figure 3) will approach an unperturbed heteroclinic orbit. For the dual-spin spacecraft, two of the dissipation mechanisms along the heteroclinic orbits are identical, thus $D_1 = D_4$ and $D_2 = D_3$ so that there are only two parameters. We assume

$$D_1 > 0, \quad D_2 < 0, \quad D_3 < 0, \quad D_4 > 0, \quad (72)$$

with Equations (68) and (69) since we show numerically this corresponds to our specific case. Interesting cases can arise if these inequalities (72) are violated with Equations (68–71) being satisfied [9].

There is a competition between three capture regions which we call left (L), middle (M), and right (R) for the cartoon shown in Figure 5. The boundaries of the basins of attraction are the stable manifolds of the saddle points, and they are sketched in Figure 6 near the

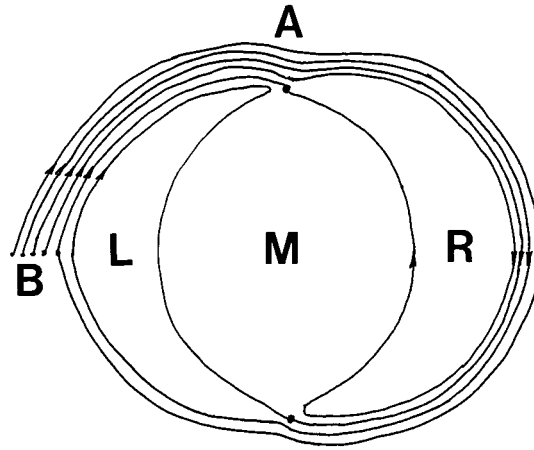


Figure 6. The stable manifolds of the saddle points (marked with dots) are the boundaries of the basins of attraction. The neighborhood of the upper saddle (marked A) is the *entrance saddle approach*. The energy w_0 that a trajectory has at A determines which capture region (L, M or R) it approaches, see Equations (73–76). The energy predicted by the method of averaging may be used at the points marked B where $\phi = [\phi_c - ((D_4/2)/(D_1 + D_4))]$, see Equation (83).

unperturbed separatrix at the frozen time T_c . Each saddle point has two branches of the stable manifold. The two saddle points give rise to four branches and thus four thin bands. There are two thin bands which approach the middle capture region. The bands alternate RMLM and repeat.

We let w_0 be the energy at the entrance saddle approach which determines which attractor the solution approaches:

$$\text{if } 0 < w_0 < \varepsilon(D_1 + D_2), \text{ then capture into R,} \tag{73}$$

$$\text{if } \varepsilon(D_1 + D_2) < w_0 < \varepsilon D_1, \text{ then capture into M,} \tag{74}$$

$$\text{if } \varepsilon D_1 < w_0 < \varepsilon(D_3 + D_4 + D_1), \text{ then capture into L,} \tag{75}$$

$$\text{if } \varepsilon(D_3 + D_4 + D_1) < w_0 < \varepsilon(D_4 + D_1), \text{ then capture into M.} \tag{76}$$

From Equations (73–76) the probability of capture is well known [17]:

$$P(R) = \frac{D_1 + D_2}{D_1 + D_4}, \tag{77}$$

$$P(L) = \frac{D_3 + D_4}{D_1 + D_4}, \tag{78}$$

$$P(M) = \frac{-D_2}{D_1 + D_4} + \frac{-D_3}{D_1 + D_4} = \frac{-D_2 - D_3}{D_1 + D_4}. \tag{79}$$

The energies (73–76) are determined by the consideration of the change in energy (66) and (67) from one saddle approach to the next. Before reaching the entrance saddle approach, all solutions consist of a repeated sequence of nearly heteroclinic orbits $D_1 D_4$. The solutions which are captured into the right capture region follow the repeated sequence of nearly

heteroclinic orbits $D_1 D_2$, while those captured by the left capture region follow the nearly heteroclinic orbit D_1 succeeded by the repeated sequence $D_4 D_3$. Solutions captured into the middle capture region have two possible sequences: D_1 followed by repeated $D_2 D_3$, and $D_1 D_4$ followed by repeated $D_3 D_2$. These sequences represent both the topological sequence of nearly heteroclinic orbits and the sequence of changes of the energy (66) from one saddle approach to the next.

8. Boundaries of the Basins of Attraction

In this section we show how to use the averaged energy and phase equations (59) and (60) to determine the boundaries of the basin of attraction even though the method of averaging is not valid near the unperturbed heteroclinic orbits. We follow the method of Bourland and Haberman [2–4] who showed how to use the averaged equations at the last saddle approach to determine the boundaries of the basin of attraction for dissipatively perturbed double-well potentials with and without slow variation. Haberman and Ho [8] extended their method to dissipatively perturbed autonomous Hamiltonian systems.

The boundaries of the basin of attraction require knowing the energy H to enough accuracy to account for $O(\varepsilon)$ terms. From the near identity transformation (40), using Equation (52) we have

$$H = e + \varepsilon \frac{1}{\omega} \int_0^\phi \{g_1 e_q + g_2 e_p + e_T\} d\phi' + O(\varepsilon^2). \quad (80)$$

The easiest places to use the method of averaging are those places where ϕ is an integer or half integer. In the dual-spin spacecraft problem such points correspond to points on the x_2 - or x_3 -axes. At these places it holds that $H = e + O(\varepsilon^2)$ and $\psi = \phi + O(\varepsilon)$. We use the averaged Equations (59), (60) in which $\omega(e, T)$ and $D(e, T)$ are given by Equations (63) and (64):

$$\frac{de}{dt} = -\varepsilon \omega(e, T) D(e, T), \quad (81)$$

$$\frac{d\phi}{dt} = \omega(e, T), \quad (82)$$

with initial condition $\phi(0) = 0$, and we will choose $e(0)$ so that the corresponding energy level corresponds to the boundary of the basin of attraction. We do not distinguish the initial energy $H(0)$ from the initial averaged energy $e(0)$ since they differ by $O(\varepsilon^2)$. From Equation (81) we compute the time $T_c = \varepsilon t_c$ at which the method of averaging predicts the unperturbed heteroclinic orbit is first reached, that is $e(T_c) = 0$. Once we know T_c , we may determine the phase ϕ_c at which $e = 0$ by using Equation (82). For a general initial condition of the form $(\phi(0) = 0, e(0) \text{ arbitrary})$, ϕ_c will in general be no integer or half-integer. That is, the averaged equations predict that an arbitrary orbit will intersect the instantaneous separatrices at a generic point.

As a motion approaches the separatrices on its way to being captured, it generally ‘circles the wagons’ many times before reaching the region of separatrix crossing. Each complete cycle around the separated regions accounts for one unit of ϕ . Thus, we may locate the relative

position of the point of separatrix crossing (as predicted by the averaged equations). We will show that it is convenient to define ϕ_c^{mod} in the following unconventional way:

$$\phi_c^{\text{mod}} = \phi_c - \frac{\frac{1}{2} D_4}{D_1 + D_4} - \left[\phi_c - \frac{\frac{1}{2} D_4}{D_1 + D_4} \right], \quad (83)$$

where ϕ_c^{mod} is the modulus (or fractional part) of the phase relative to the phase $(D_4/2)/(D_1 + D_4)$ at which solutions first approach the entrance saddle region, and

$$\left[\phi_c - \frac{\frac{1}{2} D_4}{D_1 + D_4} \right]$$

is the integer part of this phase and will be the number of oscillations before capture).

The corresponding change in the energy variable e which occurs as the motion passes through its last fraction of a cycle ϕ_c^{mod} can be obtained by approximating the energy dissipation function for the strongly nonlinear oscillator $D(e, T) \approx D_1 + D_4$ by a constant near the unperturbed heteroclinic orbit evaluated at the frozen time T_c . In this case, from Equations (81) and (82), $de/d\phi = -\varepsilon D(e, T)$, where the frozen time has been used for the frequency $\omega(e, T)$. Thus, for a partial orbit near the unperturbed heteroclinic orbit

$$\Delta e = -\varepsilon(D_1 + D_4)\Delta\phi, \quad (84)$$

where the dissipation has been approximated by a constant. Small percentage errors which have occurred are not important in this calculation because the leading order term is $O(\varepsilon)$.

Now since the average energy $e = 0$ at ϕ_c , Equation (84) gives the following expression for the energy at $[\phi_c - ((D_4/2)/(D_1 + D_4))]$:

$$H \approx e = \varepsilon(D_1 + D_4)\phi_c^{\text{mod}} + \frac{1}{2} \varepsilon D_4. \quad (85)$$

Note that the actual energy H is well approximated by the average energy e at this point where the phase is an integer by the foregoing symmetry arguments.

The energy H when the phase is an integer (85) can be related (see Figure 6) to the energy w_0 at the entrance saddle approach as follows:

$$H - w_0 = \frac{1}{2} \varepsilon D_4 \quad (86)$$

since the orbit corresponds to one half of a nearly heteroclinic orbit of the D_4 topology. Using Equation (85) for H gives

$$w_0 = \varepsilon(D_1 + D_4)\phi_c^{\text{mod}}. \quad (87)$$

Given initial conditions on the averaged energy $e(0)$ we can determine ϕ_c^{mod} and hence w_0 from Equation (87). However, Equations (73–76) show how w_0 determines which capture region the solution approaches. Thus, we can express the basins of attraction in terms of ϕ_c^{mod} which is computed from the averaged Equations (59) and (60) with initial condition $\phi(0) = 0$ (and only depends on the initial averaged energy $e(0)$):

$$\text{if } 0 < \phi_c^{\text{mod}} < \frac{D_1 + D_2}{D_1 + D_4}, \text{ then capture into R,} \quad (88)$$

$$\text{if } \frac{D_1 + D_2}{D_1 + D_4} < \phi_c^{\text{mod}} < \frac{D_1}{D_1 + D_4}, \text{ then capture into M,} \quad (89)$$

$$\text{if } \frac{D_1}{D_1 + D_4} < \phi_c^{\text{mod}} < \frac{D_3 + D_4 + D_1}{D_1 + D_4}, \text{ then capture into L,} \quad (90)$$

$$\text{if } \frac{D_3 + D_4 + D_1}{D_1 + D_4} < \phi_c^{\text{mod}} < 1, \text{ then capture into M.} \quad (91)$$

In the case of the dual-spin spacecraft, we have the symmetry $D_1 = D_4 > 0$ and $D_2 = D_3 < 0$ with $D_1 + D_2 > 0$, giving:

$$\text{if } 0 < \phi_c^{\text{mod}} < \frac{D_1 + D_2}{2D_1}, \text{ then capture into R,} \quad (92)$$

$$\text{if } \frac{D_1 + D_2}{2D_1} < \phi_c^{\text{mod}} < \frac{1}{2}, \text{ then capture into M,} \quad (93)$$

$$\text{if } \frac{1}{2} < \phi_c^{\text{mod}} < \frac{1}{2} + \frac{D_1 + D_2}{2D_1}, \text{ then capture into L,} \quad (94)$$

$$\text{if } \frac{1}{2} + \frac{D_1 + D_2}{2D_1} < \phi_c^{\text{mod}} < 1, \text{ then capture into M.} \quad (95)$$

Formulas (88–95) also correspond to the boundaries of the basin of attraction (the stable manifold of the saddle points).

9. Numerical Computations

In this section we apply the asymptotic theory developed above to the dual-spin spacecraft equations. The goal of the computation is to determine which initial conditions lead to capture into each of the three attractive regions, that is, to find the boundaries of the basins of attraction. As a check on the theory, we compare its predictions with direct numerical integration of the original differential equations of motion.

The numerical procedure may be outlined as follows:

1. Compute $\omega(e, T)$ from Equation (16).
2. Compute $D(e, T)$ from Equation (64).
3. Compute the quantities $D_1 = D_4$ and $D_2 = D_3$ from Equation (67).
4. Integrate the averaged Equation (81)

$$\frac{de}{dT} = -\omega(e, T)D(e, T), \quad (96)$$

with the initial condition $e(0) = e_0$, where e_0 is a parameter to be determined. Here e_0 , when chosen appropriately, will correspond to a boundary of a basin of attraction. Integrate Equation (97) until $e = 0$, and call that time T_c , that is $e(T_c) = 0$.

5. Integrate the averaged Equation (82)

$$\frac{d\phi}{dT} = \frac{\omega(e, T)}{\varepsilon}, \tag{97}$$

with initial condition $\phi(0) = 0$. Integrate from $T = 0$ to $T = T_c$, and call the final value ϕ_c , that is $\phi(T_c) = \phi_c$.

6. Steps 4 and 5 above will yield a value of ϕ_c for each initial condition e_0 . Vary e_0 until ϕ_c satisfies one of the conditions:

$$\phi_c^{\text{mod}} = \left\{ 0, \frac{D_1 + D_2}{2D_1}, \frac{1}{2}, \frac{1}{2} + \frac{D_1 + D_2}{2D_1}, 1 \right\}, \tag{98}$$

in which case the initial condition ($\phi(0) = 0, e(0) = e_0$) will lie on the basin boundary separating the regions {MR,RM,ML,LM,MR}, respectively. Since the basin boundaries lie close to one another, especially for smaller values of ε , the hunt for appropriate values of e_0 may involve very small increments.

7. In order to compare the predictions obtained by the foregoing calculations with direct integration of the original differential equations, proceed as follows: replace x_1 in Equations (2) and (3) by use of Equation (7). Then integrate the resulting pair of differential equations with the initial condition $x_2(0) = 0$ (corresponding to $\phi(0) = 0$), while varying $x_3(0)$ (corresponding to varying $e(0)$), until a basin boundary is reached.

We now proceed with the details. From Equation (4) we take

$$\mu = \mu_0 - T. \tag{99}$$

From Equation (16) we find

$$\frac{1}{\omega(e, T)} = \oint \frac{dx_1}{(i_2 - i_3)x_2x_3}. \tag{100}$$

In order to simplify this integral, we write Equation (8) in the form:

$$(i_2 - i_3)x_2^2 = F_2(x_1, \mu) - e, \quad \text{where} \quad F_2(x_1, \mu) = i_3x_1^2 - 2\mu x_1 + \frac{\mu^2}{i_2} + i_2 - i_3. \tag{101}$$

A similar expression for x_3^2 may be obtained by solving Equation (7) for x_2^2 and substituting in Equation (8):

$$(i_2 - i_3)x_3^2 = e - F_3(x_1, \mu), \quad \text{where} \quad F_3(x_1, \mu) = i_2x_1^2 - 2\mu x_1 + \frac{\mu^2}{i_2}. \tag{102}$$

Equation (100) becomes

$$\frac{1}{\omega(e, T)} = \oint \frac{dx_1}{F(x_1, \mu)}, \quad \text{where} \quad F(x_1, \mu) = \sqrt{F_2(x_1, \mu) - e} \sqrt{e - F_3(x_1, \mu)}. \tag{103}$$

It turns out that this integral can be evaluated in closed form [10, 13]:

$$\frac{1}{\omega(e, T)} = \frac{8}{\sqrt{i_2i_3}} \frac{K(k)}{\sqrt{(a-c)(b-d)}}, \quad \text{where} \quad k^2 = \frac{(a-b)(c-d)}{(a-c)(b-d)}, \tag{104}$$

where $K(k)$ is the complete elliptic integral of the first kind [5], and $a > b > c > d$ are roots of $F_2(x_1, \mu) - e = 0$ and $e - F_3(x_1, \mu) = 0$. Here a is always the larger root of the F_2 equation and b is always the larger root of the F_3 equation.

Next we find $D(e, T)$ from Equation (64):

$$D(e, T) = 2 \oint \frac{x_1 - \frac{\mu}{i_2}}{F(x_1, \mu)} dx_1. \quad (105)$$

This integral can also be evaluated in closed form [10, 13]:

$$D(e, T) = \frac{2}{\omega(e, T)} \left(G - \frac{\mu}{i_2} \right), \quad (106)$$

where

$$G = b + \frac{b\pi(\alpha^2 - \alpha_1^2)(1 - \Lambda(\psi, k))}{2K(k)\sqrt{\alpha^2(1 - \alpha^2)(\alpha^2 - k^2)}}, \quad (107)$$

$$\alpha^2 = \frac{a-b}{a-c}, \quad \alpha_1^2 = \frac{c}{b}\alpha^2, \quad \psi = \sin^{-1} \sqrt{\frac{1 - \alpha^2}{1 - k^2}}, \quad (108)$$

and where $\Lambda(\psi, k)$ is Heuman's Lambda function:

$$\Lambda(\psi, k) = \frac{2}{\pi} [E(k)\mathcal{F}(\psi, k') + K(k)E(\psi, k') - K(k)\mathcal{F}(\psi, k')], \quad (109)$$

where $E(k)$ is the complete elliptic integral of the second kind, $\mathcal{F}(\psi, k')$ and $E(\psi, k')$ are the incomplete elliptic integrals of the first and second kind respectively, and $k'^2 = 1 - k^2$.

Next we find D_1 and D_2 . D_1 is the D -integral (105) evaluated along one of the two exterior heteroclinic orbits connecting the saddles, and D_2 is the same integral evaluated along one of the two interior heteroclinic orbits. The D -integral simplifies along these orbits and we obtain:

$$D_1 = \frac{4}{\sqrt{i_2 i_3}} \left\{ \frac{\pi}{2} - \sin^{-1} \left(\frac{\mu \left(\frac{1}{i_2} - \frac{1}{i_3} \right)}{A} \right) \right\}, \quad (110)$$

$$D_2 = \frac{4}{\sqrt{i_2 i_3}} \left\{ -\frac{\pi}{2} - \sin^{-1} \left(\frac{\mu \left(\frac{1}{i_2} - \frac{1}{i_3} \right)}{A} \right) \right\}, \quad (111)$$

where

$$A = \sqrt{\left(1 - \frac{i_2}{i_3}\right) \left(1 - \frac{\mu^2}{i_2 i_3}\right)}. \quad (112)$$

In our numerical integrations, we follow [13] and take $i_2 = -0.3$ and $i_3 = -0.7$. We also choose $\mu_0 = 0.25$, see Equation (99). As an example of our computations, we find that for $\varepsilon = 0.001$, the initial condition $x_3(0) = -0.821034$, $x_2(0) = 0$, $x_1(0) = 0.570879$, which corresponds to energy $e(0) = -0.321905$ and phase $\phi(0) = 0$, leads to a basin boundary. We find $T_c = 0.191746$ and hence the frozen value of μ for separatrix crossing is $\mu_c = 0.058254$.

Table 1. $\varepsilon = 0.001$, $x_3(0)$ values for basin boundaries ($x_2(0) = 0$). T_c , μ_c and ϕ_c refer to separatrix crossing, as predicted by the averaged Equations (96) and (97).

Regions	$x_3(0)$ original equations	$x_3(0)$ averaged equations	$x_3(0)$ error	T_c	μ_c	ϕ_c
LM	-0.821034	-0.820697	-0.000337	0.191746	0.058254	9.836390
MR	-0.814109	-0.814138	+0.000029	0.197470	0.052530	10.25
RM	-0.813277	-0.812912	-0.000365	0.198528	0.051472	10.326922
ML	-0.806102	-0.806132	+0.000030	0.204306	0.045694	10.75
LM	-0.805437	-0.805045	-0.000392	0.205222	0.044778	10.817452

Table 2. $\varepsilon = 0.0001$, $x_3(0)$ values for basin boundaries ($x_2(0) = 0$). T_c , μ_c and ϕ_c refer to separatrix crossing, as predicted by the averaged Equations (96) and (97).

Regions	$x_3(0)$ original equations	$x_3(0)$ averaged equations	$x_3(0)$ error	T_c	μ_c	ϕ_c
LM	-0.8183775	-0.8183733	-0.0000042	0.1937874	0.0562126	99.8335524
MR	-0.8177132	-0.8177135	+0.0000003	0.1943644	0.0556350	100.25
RM	-0.8175869	-0.8175826	-0.0000043	0.1944787	0.0555213	100.3325891
ML	-0.8169202	-0.8169205	+0.0000003	0.1950563	0.0549437	100.75
LM	-0.8167953	-0.8167910	-0.0000043	0.1951691	0.0548309	100.8316258

The associated value of ϕ_c is computed to be $\phi_c = 9.836390$, while the values of D_1 and D_2 are found to be $D_1 = 15.0075$ and $D_2 = -12.4145$. Referring to Equation (98), we find

$$\frac{1}{2} + \frac{D_1 + D_2}{2D_1} = 0.58639,$$

which equals ϕ_c^{mod} , showing that the stated initial condition approximately lies on a basin boundary.

Our results are displayed in Tables 1 and 2, for $\varepsilon = 0.001$ and 0.0001 , respectively. These tables give the values of $x_3(0)$ corresponding to five consecutive basin boundaries, as shown in Figure 7. For each entry we also give the associated values of T_c , μ_c and ϕ_c . Recall that $[\phi_c]$, the integer part of ϕ_c , represents the number of complete revolutions a motion makes while approaching the heteroclinic orbits. Note that $[\phi_c]$ is around 10 or 100 for the entries in Tables 1 and 2, respectively.

In our model, once μ achieves the value of zero, the motor is turned off and μ remains zero. Since μ goes from its initial value $\mu_0 = 0.25$ to $\mu = 0$ in finite time ($= \mu_0/\varepsilon$), capture consists of entering a separated region and eventually circulating around the associated center in an $\varepsilon = 0$ periodic orbit, cf. Figure 2. In addition, some motions which start in the region surrounding the North pole, while being attracted to one of the regions L, M or R, do not get captured in the time interval before the motor is turned off. These motions remain circulating

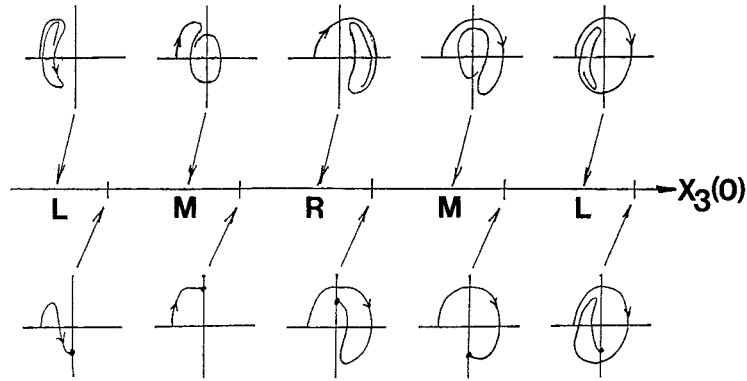


Figure 7. Sketches of orbits which correspond to captured orbits (top) and orbits which are basin boundaries (bottom) as a function of the initial condition $x_3(0)$. The other initial conditions are $x_2(0) = 0, x_1(0) = \sqrt{1 - x_3(0)^2}$ (see Tables 1 and 2). Since the orbits circle the origin many times before being captured, the initial portion of each trajectory has been omitted. Since once an orbit has been captured, it circles the associated slow-varying center many times, the final portion of each captured trajectory has also been omitted.

around the North pole. The measure of such motions goes to zero as ε goes to zero (see Figures 8 and 9).

10. Conclusions

From Tables 1 and 2 we see that the asymptotic theory agrees excellently with direct numerical integration of the original differential equations of motion. From Table 1, it can be seen that for the five entries, the total bandwidth is $0.821034 - 0.805437 \approx 0.0156$, so the maximum error of about 0.0004 is about 2.5% for $\varepsilon = 0.001$. The comparable calculation for $\varepsilon = 0.0001$ is, from Table 2, about one-tenth as much. This excellent agreement should not be unexpected since the asymptotics constitute a second order theory. This is true in spite of the fact that only the lowest order terms are maintained! The explanation for this is that because of symmetry, the second order terms vanish, making what would normally be a first order theory valid to second order. To see this, compare Equations (45) and (46) with Equations (59) and (60). The symmetry requirement is met by the dual-spin spacecraft equations, but, in addition, it is required that the symmetric initial condition $x_2(0) = 0$ be invoked.

The theoretical results for the probabilities of capture given in Equations (77–79) agree quite well with the numerical computations. Using a representative value of $\mu = 0.05$, Equations (110–112) give $D_1 = D_4 = 14.82$ and $D_2 = D_3 = -12.60$ from which we obtain the theoretical probabilities of capture $P(M) = 85.0\%$, $P(L) = P(R) = 7.5\%$. The numerical computation for the probabilities of capture are obtained by computing ratios of the changes in the initial values of $x_3(0)$ in the last five entries in Tables 1 and 2. There are four bands, two Ms, one L and one R. For $\varepsilon = 0.001$ we obtain $P(M) = 90.4\%$, $P(L) = 5.3\%$, $P(R) = 4.3\%$, whereas for $\varepsilon = 0.0001$ we obtain $P(M) = 84.1\%$, $P(L) = 8.0\%$, $P(R) = 7.9\%$. Note that the agreement with theory is better for the smaller value of ε . Also note that these probability computations assume that the initial conditions lie in the region of phase space filled by the alternating bands which encircle the L, M and R capture regions, cf. Figure 8.

Although the asymptotic method presented in this paper improves our understanding of the dynamics of resonant capture, we were not able to express our final results in analytic form.

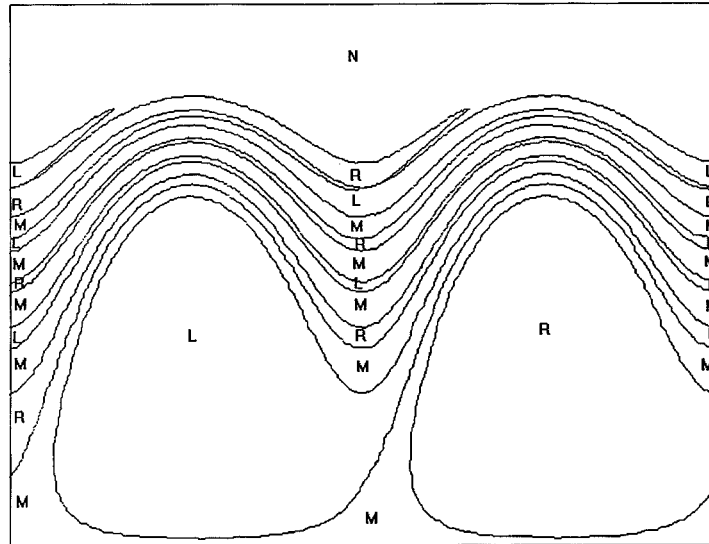


Figure 8. Regions of attraction as obtained by numerical integration of Equations (1–4). Parameters are $\varepsilon = 0.005$, $i_2 = -0.3$, $i_3 = -0.7$, $\mu_0 = 0.25$. Letters represent capture regions: L = Left, R = Right, M = Middle (South pole), N = North pole. In order to better see the continuity of the regions, the unit sphere (7) has been punctured at the North and South poles, then opened up into a cylinder, and finally unrolled. The vertical axis is x_1 , going from -1 to 1 . The horizontal axis is $\arctan(x_2/x_3)$ going from $-3\pi/2$ to $\pi/2$. E.g., a point lying in a region marked L means that a motion with the corresponding initial condition is captured into the left capture region. Motions in region N, while being attracted to one of the regions L, M or R, have not had enough time to be captured in the time interval μ_0/ε , before the motor is turned off at $\mu = 0$.

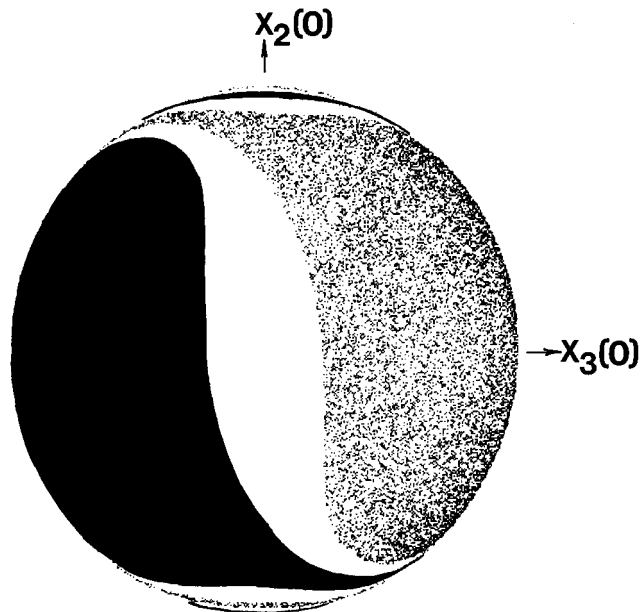


Figure 9. Basins of attraction in initial condition space. The data of Figure 8 is here displayed as a projection of the bottom half of the sphere (7) from infinity onto the $x_3(0) - x_2(0)$ plane. Initial conditions in the white, black and dotted regions are attracted respectively to capture regions M, L and R. Results obtained by numerical integration of Equations (1–4). Parameters are $i_2 = -0.3$, $i_3 = -0.7$, $\varepsilon = 0.005$, $\mu_0 = 0.25$.

In general, there are two barriers to obtaining closed form expressions for the critical initial conditions leading to the basin boundaries. Firstly, the integrals occurring in the averaged equations, namely Equation (61) for $\omega(e, T)$ and Equation (64) for $D(e, T)$, as well as the Melnikov integrals, Equation (67) for the quantities D_i , need to be evaluated. We were able to do this in closed form using elliptic integrals. Secondly, the resulting averaged equations, Equations (59) and (60), need to be integrated to obtain the time of separatrix crossing, T_c and associated phase ϕ_c . We were not able to do this in closed form, and used numerical integration instead.

Previous studies of this problem [11, 13, 26] have noted the key difficulty of dealing with the crossing of the slowly moving separatrices. The present work offers a solution to these difficulties by supplementing the averaged equations with energy changes represented by Melnikov integrals in the neighborhood of the slowly moving separatrices. This results in a clear understanding of how the question of capture is influenced by the phase ϕ_c which a motion has when it reaches the instantaneous separatrix.

Acknowledgement

Author RR wishes to thank Professor Chris Hall for helpful discussions.

Appendix A: Change of Variables

Various expressions in this appendix are well known change of variables formulas from (q, p, T) to (H, ψ, T) . Since $H = H(q, p, T)$, by taking partial derivatives with respect to H, ψ, T , we obtain

$$1 = H_q q_H + H_p p_H, \tag{113}$$

$$0 = H_q q_\psi + H_p p_\psi, \tag{114}$$

$$0 = H_q q_T + H_p p_T + H_T. \tag{115}$$

There are similar expressions following from $\psi = \psi(q, p, T)$:

$$0 = \psi_q q_H + \psi_p p_H, \tag{116}$$

$$1 = \psi_q q_\psi + \psi_p p_\psi, \tag{117}$$

$$0 = \psi_q q_T + \psi_p p_T + \psi_T. \tag{118}$$

Since $H = H(q, p, T)$,

$$\frac{dH}{dt} = H_q \frac{dq}{dt} + H_p \frac{dp}{dt} + \varepsilon H_T. \tag{119}$$

Using Equations (10), (11), (17), (18), and (114), this becomes Equation (19):

$$\frac{dH}{dt} = \varepsilon(g_1 H_q + g_2 H_p + H_T). \tag{120}$$

A similar expression for $d\psi/dt$ using Equation (117) yields Equation (20):

$$\frac{d\psi}{dt} = \omega(\mathbf{H}, T) + \varepsilon(g_1\psi_q + g_2\psi_p + \psi_T). \quad (121)$$

Although Equations (120) and (121) will be satisfactory for our purposes, they are somewhat incomplete from a theoretical and practical point of view since we wish to express our functions as functions of \mathbf{H} and ψ , where we assume we have been successful in determining q and p as functions of \mathbf{H} and ψ . We write a few additional formulas (which we do not use in this paper and are particularly well known for Hamiltonian systems) in order to express Equations (120) and (121) as functions of \mathbf{H} and ψ . The Jacobian of the transformation can be determined using Equations (17), (18), (12), (13) and (113):

$$q_\psi p_{\mathbf{H}} - p_\psi q_{\mathbf{H}} = \frac{f_1 p_{\mathbf{H}} - f_2 q_{\mathbf{H}}}{\omega} = \frac{\gamma}{\omega} (\mathbf{H}_p p_{\mathbf{H}} + \mathbf{H}_q q_{\mathbf{H}}) = \frac{\gamma}{\omega}. \quad (122)$$

Individual partial derivatives can now be determined from Equations (113–115):

$$\mathbf{H}_p = \frac{\omega q_\psi}{\gamma}, \quad \mathbf{H}_q = -\frac{\omega p_\psi}{\gamma}, \quad \mathbf{H}_T = -(\mathbf{H}_q q_T + \mathbf{H}_p p_T) = \frac{\omega}{\gamma} (p_\psi q_T - q_\psi p_T), \quad (123)$$

and from Equations (115) and (116):

$$\psi_p = -\frac{\omega q_{\mathbf{H}}}{\gamma}, \quad \psi_q = \frac{\omega p_{\mathbf{H}}}{\gamma}, \quad \psi_T = -(\psi_q q_T + \psi_p p_T) = \frac{\omega}{\gamma} (-p_{\mathbf{H}} q_T + q_{\mathbf{H}} p_T). \quad (124)$$

Since \mathbf{H} is known explicitly but ψ is not, these may be treated differently. These expressions are similar to those derived in [2, 8].

Appendix B: Near-Identity Transformation for Averaging

In this appendix we derive Equations (42) and (43). Using the chain rule on Equations (38) and (39),

$$\frac{d}{dt} \begin{bmatrix} \mathbf{H} \\ \psi \end{bmatrix} = [\mathbf{I} + \varepsilon \mathbf{A}] \frac{d}{dt} \begin{bmatrix} e \\ \phi \end{bmatrix} + \begin{bmatrix} \varepsilon^2 \mathbf{H}_{1T} + \dots \\ \varepsilon^2 \psi_{1T} + \dots \end{bmatrix}, \quad (125)$$

where

$$\varepsilon \mathbf{A} = \begin{bmatrix} \varepsilon \mathbf{H}_{1e} + \varepsilon^2 \mathbf{H}_{2e} + \dots & \varepsilon \mathbf{H}_{1\phi} + \varepsilon^2 \mathbf{H}_{2\phi} + \dots \\ \varepsilon \psi_{1e} + \varepsilon^2 \psi_{2e} + \dots & \varepsilon \psi_{1\phi} + \varepsilon^2 \psi_{2\phi} + \dots \end{bmatrix}. \quad (126)$$

Solving for $d/(dt) \begin{bmatrix} e \\ \phi \end{bmatrix}$, we obtain

$$\frac{d}{dt} \begin{bmatrix} e \\ \phi \end{bmatrix} = [\mathbf{I} + \varepsilon \mathbf{A}]^{-1} \left\{ \frac{d}{dt} \begin{bmatrix} \mathbf{H} \\ \psi \end{bmatrix} - \begin{bmatrix} \varepsilon^2 \mathbf{H}_{1T} + \dots \\ \varepsilon^2 \psi_{1T} + \dots \end{bmatrix} \right\}. \quad (127)$$

The near identity matrix is easily inverted, $[\mathbf{I} + \varepsilon \mathbf{A}]^{-1} = \mathbf{I} - \varepsilon \mathbf{A} + \varepsilon^2 \mathbf{A}^2 - \dots$, and the standard form is used to evaluate $d/(dt) \begin{bmatrix} \mathbf{H} \\ \psi \end{bmatrix}$:

$$\frac{d}{dt} \begin{bmatrix} e \\ \phi \end{bmatrix} = [\mathbf{I} - \varepsilon \mathbf{A} + \varepsilon^2 \mathbf{A}^2] \begin{bmatrix} \varepsilon f(\mathbf{H}, \psi, T) \\ \omega(\mathbf{H}, T) + \varepsilon g(\mathbf{H}, \psi, T) \end{bmatrix} - \varepsilon^2 \begin{bmatrix} \mathbf{H}_{1T} \\ \psi_{1T} \end{bmatrix} + \mathbf{O}(\varepsilon^3). \quad (128)$$

For our purposes, we already have sufficient information from Equation (128) concerning the angle ϕ , namely

$$\frac{d\phi}{dt} = \omega(H, T) + \varepsilon g(H, \psi, T) - \varepsilon \omega(H, T) \psi_{1\phi} + O(\varepsilon^2). \quad (129)$$

Shortly, we will be more precise concerning Equation (129) since H and ψ are on the right-hand side of Equation (129). We have to work harder to obtain the accurate information we need concerning e . The leading-order part of $\varepsilon^2 \mathbf{A}^2$ follows from Equation (126), but we will actually only need one entry of the following:

$$\varepsilon^2 \mathbf{A}^2 = \varepsilon^2 \begin{bmatrix} H_{1e}^2 + H_{1\phi} \psi_{1e} & H_{1\phi} (H_{1e} + \psi_{1\phi}) \\ \psi_{1e} (H_{1e} + \psi_{1\phi}) & H_{1\phi} \psi_{1e} + \psi_{1\phi}^2 \end{bmatrix} + \mathbf{O}(\varepsilon^3). \quad (130)$$

Thus, from Equation (128) we obtain

$$\begin{aligned} \frac{de}{dt} = & \varepsilon f(H, \psi, T) - \varepsilon \omega(H, T) H_{1\phi} - \varepsilon^2 \omega(H, T) H_{2\phi} - \varepsilon^2 f(H, \psi, T) H_{1e} \\ & - \varepsilon^2 g(H, \psi, T) H_{1\phi} + \varepsilon^2 \omega(H, T) H_{1\phi} (H_{1e} + \psi_{1\phi}) - \varepsilon^2 H_{1T} + O(\varepsilon^3). \end{aligned} \quad (131)$$

We use the near identity transformation (40) and (41) to relate the old variables to the new ones, so that using Taylor series we obtain

$$\omega(H, T) = \omega(e, T) + \varepsilon \omega_e(e, T) H_1(e, \phi, T) + O(\varepsilon^2), \quad (132)$$

$$f(H, \psi, T) = f(e, \phi, T) + \varepsilon (f_e H_1 + f_\phi \psi_1) + O(\varepsilon^2), \quad (133)$$

where all expressions are now in terms of the new variables e and ϕ . A similar expression for g exists. When Equations (132) and (133) are substituted into Equations (129) and (131), we obtain Equations (42) and (43).

References

1. Arnold, V. I., Kozlov, V. V., and Neishtadt, A. I., *Mathematical Aspects of Classical and Celestial Mechanics, Dynamical Systems III*, Springer-Verlag, New York, 1988.
2. Bourland, F. J. and Haberman, R., 'Separatrix crossing: Time-invariant potentials with dissipation', *SIAM Journal of Applied Mathematics* **50**, 1990, 1716–1744.
3. Bourland, F. J. and Haberman, R., 'Capture and the connection formulas for the transition across a separatrix', in *Asymptotic Analysis and the Numerical Solution of Partial Differential Equations*, H. G. Kaper and M. Garbey (eds.), Dekker, New York, 1991, pp. 17–30.
4. Bourland, F. J., Haberman, R., and Kath, W. L., 'Averaging methods for the phase shift of arbitrarily perturbed strongly nonlinear oscillators with an application to capture', *SIAM Journal of Applied Mathematics* **51**, 1991, 1150–1167.
5. Byrd, P. F. and Friedman, M. D., *Handbook of Elliptic Integrals for Engineers and Scientists*, 2nd ed., Springer-Verlag, Berlin, 1971.
6. Guckenheimer, J. and Holmes, P., *Nonlinear Oscillations, Dynamical Systems, and Bifurcations of Vector Fields*, Springer-Verlag, New York, 1983.
7. Haberman, R., 'Energy bounds for the slow capture by a center in sustained resonance', *SIAM Journal of Applied Mathematics* **43**, 1983, 244–256.
8. Haberman, R. and Ho, E. K., 'Boundary of the basin of attraction for weakly damped primary resonance', *Journal of Applied Mechanics* **62**, 1995, 941–946.
9. Haberman, R. and Rand, R. H., 'Sequences of orbits and the boundaries of the basin of attraction for two double heteroclinic orbits', submitted for publication.

10. Hall, C. D., 'An investigation of spinup dynamics of axial gyrostats using elliptic integrals and the method of averaging', Ph.D. Thesis, Department of Theoretical and Applied Mechanics, Cornell University, Ithaca, NY, 1992.
11. Hall, C. D., 'Resonance capture in axial gyrostats', *Journal of the Astronautical Sciences* **43**, 1995, 127–138.
12. Hall, C. D., 'Momentum transfer in torque-free gyrostats', in *Nonlinear Dynamics: The Richard Rand 50th Anniversary Volume*, A. Guran (ed.), World Scientific, Singapore, 1997, pp. 60–88.
13. Hall, C. D. and Rand, R. H., 'Spinup dynamics of axial dual-spin spacecraft', *Journal of Guidance, Control, and Dynamics* **17**, 1994, 30–37.
14. Hughes, P. C., *Spacecraft Attitude Dynamics*, Wiley, New York, 1986.
15. Kinsey, R. J., Mingori, D. L., and Rand, R. H., 'Spinup through resonance of rotating unbalanced systems with limited torque', in *Proceedings of the 1990 AIAA/AAS Astrodynamics Conference*, Part 2, AIAA Paper No. AIAA-90-2966, AIAA, Washington, DC, 1990, pp. 805–813.
16. Kinsey, R. J., Mingori, D. L., and Rand, R. H., 'Nonlinear control of a dual-spin spacecraft during despin through precession phase lock', *Journal of Guidance, Control, and Dynamics* **19**, 1996, 60–67.
17. Neishtadt, A. I., 'Probability phenomena due to separatrix crossing', *Chaos* **1**, 1991, 42–48.
18. Quinn, D., Rand, R., and Bridge, J., 'The dynamics of resonant capture', *Nonlinear Dynamics* **8**, 1995, 1–20.
19. Rand, R. H., *Topics in Nonlinear Dynamics with Computer Algebra*, Gordon and Breach, Langhorne, PA, 1994.
20. Rand, R. H. and Armbruster, D., *Perturbation Methods, Bifurcation Theory and Computer Algebra*, Springer-Verlag, New York, 1987.
21. Rand, R. H., Kinsey, R. J., and Mingori, D. L., 'Dynamics of spinup through resonance', *International Journal of Non-Linear Mechanics*, **27**, 1992, 489–502.
22. Robinson, C., 'Sustained resonance for a nonlinear system with slowly varying coefficients', *SIAM Journal Mathematical Analysis* **14**, 1983, 847–860.
23. Sanders, J. A. and Verhulst, F., *Averaging Methods in Nonlinear Dynamical Systems*, Springer-Verlag, New York, 1985.
24. Tennyson, J. L., Cary, J. R., and Escande, D.F., 'Change of the adiabatic invariant due to separatrix crossing', *Physical Review Letters* **56**, 1986, 2117–2120.
25. Timofeev, A. V., 'On the constancy of an adiabatic invariant when the nature of the motion changes', *Zhurnal Eksperimental'noi i Teoreticheskoi Fiziki* **75**, 1978, 1303–1308 [in Russian], *Soviet Physics JETP* **48**, 1978, 656–659.
26. Tsui, R. and Hall, C. D., 'Resonance capture in unbalanced dual-spin spacecraft', *Journal of Guidance, Control, and Dynamics* **18**, 1995, 1329–1335.